

## Distribution of Magnetic Moments in Pd-3d and Ni-3d Alloys\*

J. W. CABLE, E. O. WOLLAN, AND W. C. KOEHLER

*Solid State Division, Oak Ridge National Laboratory, Oak Ridge, Tennessee*

(Received 7 December 1964)

Neutron-scattering and magnetization measurements were made on a series of face-centered cubic Pd-3d and Ni-3d alloys to determine the distribution of magnetic moments in these ferromagnetic binary alloys. The specific alloys studied were: Ni<sub>3</sub>Co, NiCo, Pd<sub>3</sub>Co, PdCo, Pd<sub>3</sub>Fe (ordered and disordered), PdFe, Pd<sub>0.93</sub>Fe<sub>0.07</sub>, and Pd<sub>0.97</sub>Fe<sub>0.03</sub>. Magnetic moments of about 3.0, 1.8, and 0.6 Bohr magnetons per atom were found for Fe, Co, and Ni, respectively, and these were essentially independent of concentration. The average Pd moment varies with concentration and approaches a maximum of about 0.4 Bohr magnetons per atom in the concentrated alloys.

### INTRODUCTION

THE paramagnetic behavior of pure Pd is drastically affected by the addition of the 3d transition metals. The alloys with Cr and Mn exhibit antiferromagnetic tendencies<sup>1</sup> while those with<sup>2</sup> Fe and<sup>3</sup> Co become ferromagnetic at very low 3d concentrations. In the dilute Fe and Co alloys the saturation moments are so large that it is necessary to assume the development of magnetic moments associated with the Pd atoms. The interpretation of the bulk magnetic data is complicated by the presence of this induced moment, so that the determination of individual atomic magnetic moments by neutron-diffraction measurements is important to a better understanding of these systems. This investigation was undertaken to determine the distribution of magnetic moments in such alloys and in some of the corresponding Ni alloys. Some of the results contained herein have appeared in abbreviated form,<sup>4,5,6</sup> but are included in the interest of completeness.

### EXPERIMENTAL

The alloys included in this study were: Ni<sub>3</sub>Co, NiCo, Pd<sub>3</sub>Co, PdCo, PdFe, Pd<sub>3</sub>Fe, Pd<sub>0.93</sub>Fe<sub>0.07</sub>, and Pd<sub>0.97</sub>Fe<sub>0.03</sub>. The samples were prepared by arc melting of appropriate amounts of the constituents. The con-

centrated alloys were heat treated by stepwise cooling from about 900°C to room temperature over a period of about 12 days. After this treatment, Pd<sub>3</sub>Fe and PdFe showed the effects of long-range positional order; the PdCo alloys exhibited short-range order, and the NiCo alloys showed neither short-range- nor long-range-order effects.

Magnetization measurements were made by the ballistic method with fields up to 5 kOe. A nickel standard was used for calibration, and saturation moments were obtained by matching slopes with the Ni curve at the higher field values. Measurements were made at 298 and 77°K for the concentrated alloys and from 4.2 to 150°K for the dilute Fe in Pd alloys. The saturation moments, corrected to 0°K by means of a Brillouin extrapolation through the low-temperature data, are given in Tables I-III. These values are in good agreement with those previously reported.<sup>2,3,7</sup>

Two types of neutron diffraction measurements were made; intensity of magnetic diffuse scattering from the ferromagnetic disordered alloys and of the coherent Bragg scattering from ordered Pd<sub>3</sub>Fe. The magnetic and nuclear scattering were separated by the application of a 12 kOe magnetic field parallel to the scattering vector. This was sufficient to extinguish the magnetic scattering which was then measured by taking the

TABLE I. Atomic magnetic moments in NiCo and Ni<sub>3</sub>Co.

Alloy	$\sigma_s(\mu_B/\text{atom})$	$d\sigma/d\Omega^a$	$ \mu_{\text{Co}} - \mu_{\text{Ni}} $	$\mu_{\text{Co}}$	$\mu_{\text{Ni}}$
Ni <sub>3</sub> Co	0.89±0.02	0.0145±0.010	1.26±0.04	1.84±0.05 -0.05±0.05 or	0.58±0.02 1.21±0.02
NiCo	1.14±0.02	0.0152±0.010	1.12±0.04	1.70±0.03 0.58±0.03 or	0.58±0.03 1.70±0.03

<sup>a</sup> Extrapolated to the forward direction.

\* Research sponsored by the U. S. Atomic Energy Commission under contract with the Union Carbide Corporation.

<sup>1</sup> D. Gerstenberg, Ann. Physik 2, 236 (1958).

<sup>2</sup> J. Crangle, Phil. Mag. 5, 335 (1960).

<sup>3</sup> R. M. Bozorth, P. A. Wolff, D. D. Davis, V. B. Compton, and J. H. Wernick, Phys. Rev. 122, 1157 (1961).

<sup>4</sup> E. O. Wollan, J. W. Cable, W. C. Koehler, and M. K. Wilkinson, J. Phys. Soc. Japan 17, Suppl. B III, 38 (1962).

<sup>5</sup> J. W. Cable, E. O. Wollan, W. C. Koehler, and M. K. Wilkinson, J. Appl. Phys. Suppl. 33, 1340 (1962).

<sup>6</sup> J. W. Cable, E. O. Wollan, and W. C. Koehler, J. Appl. Phys. 34, 1189 (1963).

<sup>7</sup> J. J. Went, Physica 17, 98 (1951).

TABLE II. Atomic magnetic moments in Pd<sub>3</sub>Co and PdCo.

Alloy	$\sigma_s$ ( $\mu_B$ /atom)	$\mu_{Co}^a$	$d\sigma/d\Omega^b$	$\mu_{Co} - \mu_{Pd}$	$\mu_{Co}$	$\mu_{Pd}$
Pd <sub>3</sub> Co	$0.84 \pm 0.02$	$1.9 \pm 0.2$	$0.019 \pm 0.003$	$1.45 \pm 0.12$	$1.92 \pm 0.11$	$0.48 \pm 0.03$
PdCo	$1.16 \pm 0.03$	$2.0 \pm 0.1$	$0.032 \pm 0.004$	$1.63 \pm 0.10$	$1.97 \pm 0.07$	$0.35 \pm 0.07$

<sup>a</sup> From the high-angle scattering data assuming no Pd contribution and the metallic Co form factor.

<sup>b</sup> Extrapolated to  $\sin\theta/\lambda = 0$ .

TABLE III. Atomic magnetic moments in Pd-Fe alloys.

% Fe	$\sigma_s$ ( $\mu_B$ /atom)	$\mu_{Fe}^a$	$d\sigma/d\Omega^b$	$\mu_{Fe} - \mu_{Pd}$	$\mu_{Fe}$	$\mu_{Pd}$
3	$0.234 \pm 0.007$	$2.9 \pm 0.3$	$0.012 \pm 0.001$	$2.92 \pm 0.15$	$3.07 \pm 0.15$	$0.15 \pm 0.01$
7	$0.457 \pm 0.014$	$3.0 \pm 0.2$	$0.024 \pm 0.002$	$2.76 \pm 0.11$	$3.02 \pm 0.11$	$0.26 \pm 0.02$
25	$1.00 \pm 0.03$	$2.9 \pm 0.2$	$0.063 \pm 0.007$	$2.64 \pm 0.15$	$2.98 \pm 0.15$	$0.34 \pm 0.05$
50	$1.60 \pm 0.05$	$3.0 \pm 0.1$	$0.075 \pm 0.007$	$2.49 \pm 0.11$	$2.85 \pm 0.08$	$0.35 \pm 0.08$

<sup>a</sup> From the high-angle scattering data assuming no Pd contribution and the metallic Fe form factor.

<sup>b</sup> Extrapolated to  $\sin\theta/\lambda = 0$ .

difference in scattering with the field applied and removed. The intensities were calibrated with a standard Ni sample. Most of the data were obtained at room temperature and corrected to 0°K by utilizing the magnetization data.

### DISORDERED ALLOYS

#### Ni-Co Alloys

Neutron data were obtained for 25% and 50% Co alloys. Samples were in the form of heat-treated polycrystalline rods and the cold-worked filings from those rods. There was no indication of ordering, either short range or long range, for either type of sample. The observed differential cross sections for the magnetic diffuse scattering from these samples are given in Fig. 1. This cross section has the form

$$d\sigma/d\Omega = 0.0483n_1n_2(\mu_1f_1 - \mu_2f_2)^2,$$

in which the  $n$ 's are the mole fractions, the  $\mu$ 's the atomic magnetic moments, and the  $f$ 's the magnetic form factors of the constituent atoms. These data are readily extrapolated to the forward direction, where the form factor becomes unity, and yield the square of the

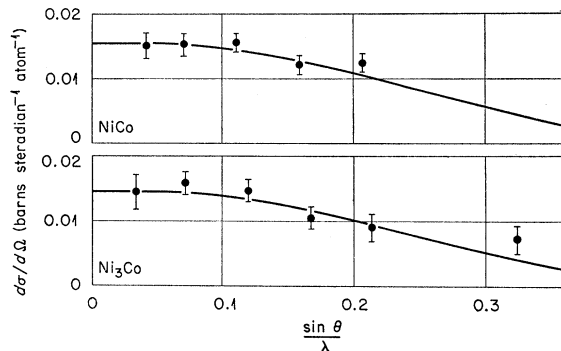


FIG. 1. Magnetic diffuse scattering cross sections for Ni<sub>3</sub>Co and NiCo.

difference in moments of the two types of atoms. This result, combined with the average moment per atom from the bulk-magnetization data, yields two alternative sets of individual atomic magnetic-moment values. The results are presented in Table I in which  $\sigma_s$  is the saturation magnetization in Bohr magnetons per atom,  $d\sigma/d\Omega$  is the differential cross section for magnetic diffuse scattering in barns per steradian per atom in the forward direction, and the  $\mu$ 's are the atomic magnetic moments. The first set of atomic-moment values is preferred because those values are close to the values for the pure metals and because the large changes in band structure necessary to produce the second set of moment values are not expected for alloys of neighboring elements. The first set is also favored by comparison with the results for the Pd-Co alloys for which unique moment values are obtained.

#### Pd-Co Alloys

The magnetic-diffuse-scattering cross sections for the two Pd-Co alloys are shown in Fig. 2. The angular dependences of these cross sections are not the smoothly varying curves appropriate to random alloys, but show structure characteristic of short-range order. In the

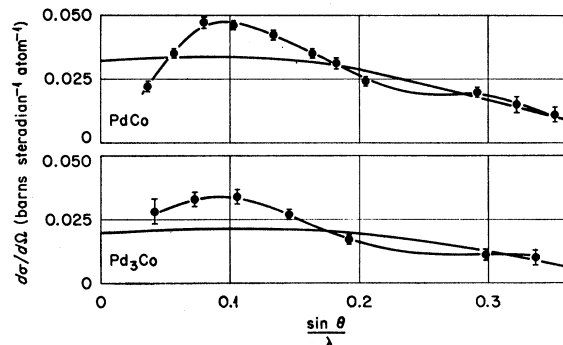


FIG. 2. Magnetic diffuse scattering cross sections for Pd<sub>3</sub>Co and PdCo.

Pd<sub>3</sub>Co case the amount of structure was dependent on sample history, being greater for the heat treated rod than for the filings which had been annealed at 1000°C for 2 h and then quenched. This indicates that the short-range order is of the positional type. The presence of this short-range order complicates the analysis of the data because of the uncertainty in the extrapolation procedure. There is, however, a compensating element in the analysis, this being the form-factor differences between Pd and the 3d metals. Because of the larger radial extent of the 4d shell relative to the 3d, the Pd form factor decreases with increasing scattering angle much more rapidly than the 3d form factors so that, in the region of  $\sin\theta/\lambda=0.3$ , the magnetic scattering is essentially from the 3d metals only. These data, along with assumed form factors, yield directly the magnetic moments of the 3d atoms. Moment values for the two Co alloys obtained by this procedure with the experimental Co form factor<sup>8</sup> are given in Column 3 of Table II. The Pd moments could be determined from the average moment values with the use of these Co moments, but these have not been listed in the table. Instead the individual moment values were refined by making use of the small-angle scattering data. The Co moments obtained from the high-angle data were used as a starting point, and random alloy-cross-section curves were calculated based on the experimental Co form factor,<sup>8</sup> the calculated Pd form factor,<sup>9</sup> and moment values consistent with the magnetization data. The median of an envelope of smooth curves about which the data executed a damped oscillation was selected as the best solution. Such curves are shown in Fig. 2, and the forward-angle cross sections are given in Column 4 of Table II. The corresponding moment differences in Column 5 do not have the usual sign ambiguity because the Co atoms were shown to have the higher moments by the high-angle data. The last two columns give the individual magnetic moments obtained by combining these moment differences with

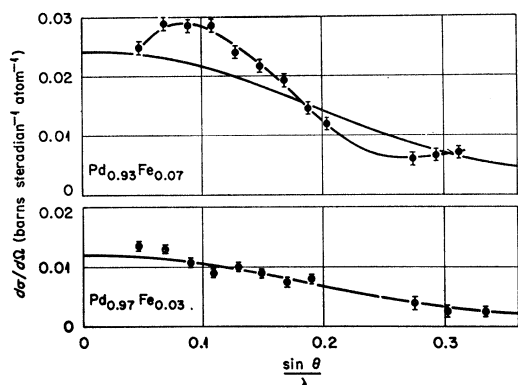


FIG. 3. Magnetic diffuse scattering cross sections for Pd<sub>0.97</sub>Fe<sub>0.03</sub> and Pd<sub>0.93</sub>Fe<sub>0.07</sub>.

<sup>8</sup> R. Nathans and A. Paoletti, Phys. Rev. Letters 2, 254 (1959).

<sup>9</sup> L. Pauling and J. Sherman, Z. Krist. 81, 1 (1932).

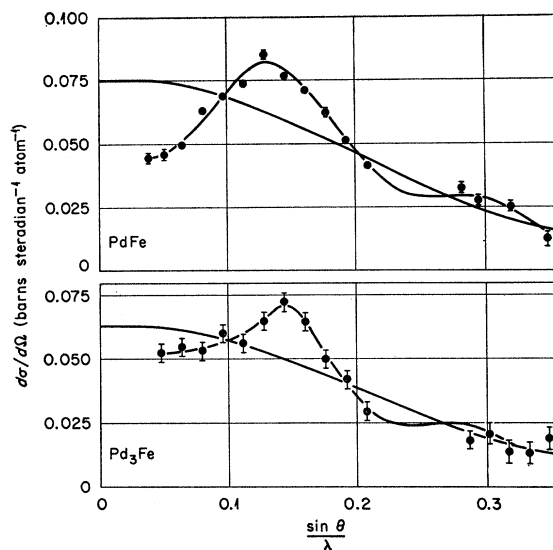


FIG. 4. Magnetic diffuse scattering cross sections for Pd<sub>3</sub>Fe and PdFe.

the average moments in Column 2. The agreement between Columns 3 and 6 supports the validity of the form-factor assumptions and the extrapolation procedure used in analyzing the small-angle data.

#### Pd-Fe Alloys

In this system, four alloys containing 3%, 7%, 25%, and 50% Fe were studied. For the two dilute alloys the samples were machined polycrystalline rods of  $\frac{1}{4}$ -in. diam that had been annealed at 1000°C for 2 h and then quenched. Neutron data were taken at 50 and 77°K, respectively, for the 3% and 7% alloys, the corresponding Curie temperatures being 114 and 200°K. The data, corrected to absolute zero by means of the 4.2°K bulk magnetization measurements, are shown in Fig. 3. For the more concentrated alloys long-range positional order was observed for the heat-treated samples. This long-range order was destroyed by mechanical filing and the filed samples were used for these diffuse scattering measurements. These cold-worked samples exhibited short-range order effects similar to the Pd-Co alloys as can be seen by reference to Fig. 4. For the 25% alloy this short-range order effect was considerably enhanced by annealing the filed sample. These data were analyzed in the same manner as the Pd-Co data with the use of the experimental Fe form factor.<sup>10</sup> The Fe moments obtained from the high-angle scattering data are listed in Column 3 of Table III while the best random alloy cross-section curves are shown in Figs. 3 and 4. The refined Fe moment values agree well with those values obtained from the high-angle data, again supporting the analytical procedure used for the small-angle data.

<sup>10</sup> R. Nathans, C. G. Shull, G. Shirane, and A. Andresen, J. Phys. Chem. Solids 10, 138 (1959).

It should be noted that, in this analysis, unique magnetic moments for the Fe and Pd atoms have been assumed. In these alloys, for which the Pd moment appears to be induced by the Fe impurity atoms, one might expect the Pd moments to vary with environment and specifically to decrease with increasing distance from the Fe atoms. Such a variation should produce structure in the cross-section curves. This would have been obscured in the 7%, 25%, and 50% alloys by the positional short-range order effect, but neither was it detected in the 3% alloy which showed no positional short-range order and for which the Pd moment variation should have been the most pronounced. Nevertheless, it is likely that this moment variation does occur and the Pd moments listed in Table III for the 3% and 7% alloys should be regarded as average values determined mainly from the bulk magnetization data by use of Fe moments established from the neutron data.

### Ordered Pd<sub>3</sub>Fe

This alloy undergoes an order-disorder transition at about 1070°K.<sup>11</sup> The Curie temperature of 540°K and the saturation moment of 1.09  $\mu_B$  per atom for the ordered alloy are both about 9% higher than for the disordered alloy. The sample was heat treated in the manner previously described and neutron diffraction data were taken at room temperature. Some of the data are shown in Fig. 5. The lower pattern in this figure was obtained with a 12-kOe field applied parallel to the scattering vector and therefore represents the nuclear scattering. The superlattice reflections have intensities which correspond to a long-range order parameter of 0.87. The upper part of the figure shows the difference

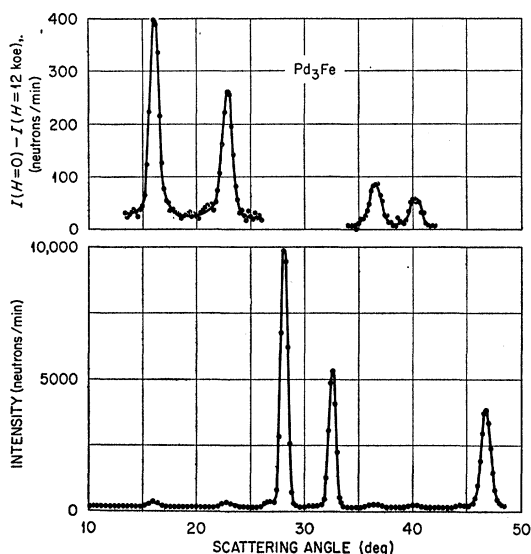


FIG. 5. Neutron diffraction patterns for ordered Pd<sub>3</sub>Fe.

<sup>11</sup> M. Hansen, *Constitution of Binary Alloys* (McGraw-Hill Book Company, Inc., New York, 1958), p. 696.

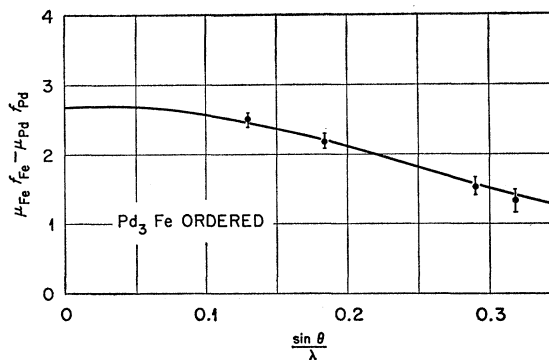


FIG. 6. Magnetic-scattering amplitudes (expressed in effective moments) for the superlattice reflections of ordered Pd<sub>3</sub>Fe.

in scattering with zero field and with the field applied, and represents the magnetic scattering from the unmagnetized sample. The intensities of these reflections were normalized to the nuclear superlattice reflection intensities with the scattering amplitudes  $b_{Fe}=0.96 \times 10^{-12}$  and  $b_{Pd}=0.60 \times 10^{-12}$  cm. The resultant magnetic scattering amplitudes, corrected to 0°K and expressed in terms of  $\mu_{Fe}f_{Fe}-\mu_{Pd}f_{Pd}$ , are given in Fig. 6. Here again, the rapid falloff of the Pd form factor proves useful in the analysis of the data. On the assumption of negligible Pd scattering for the two high-angle points along with the experimental Fe form factor, these data yield an Fe moment of  $2.9 \pm 0.2 \mu_B$ . The two smaller angle data points, however, favor a somewhat higher value as indicated by the smooth curve in Fig. 5 which corresponds to 3.1  $\mu_B$  per Fe and 0.42  $\mu_B$  per Pd.

### DISCUSSION

There is a striking similarity between the distribution of magnetic moments in these Pd-3d alloys and in the corresponding Ni-3d alloys. This is illustrated in Table IV in which the results of this study as well as some previous results<sup>12,13,14</sup> on the Ni-Fe system are presented. The most remarkable part of this series of observations

TABLE IV. Summary of atomic magnetic-moment values for Pd-Fe, Pd-Co, Ni-Fe, and Ni-Co alloys.

	$\mu_{Fe, Co}$	$\mu_{Pd}$		$\mu_{Fe, Co}$	$\mu_{Ni}$
Pd <sub>0.97</sub> Fe <sub>0.03</sub>	3.07	0.15	Ni <sub>0.985</sub> Fe <sub>0.015</sub> <sup>a</sup>	2.8	0.6
Pd <sub>0.93</sub> Fe <sub>0.07</sub>	3.02	0.26	Ni <sub>0.90</sub> Fe <sub>0.10</sub> <sup>b</sup>	2.58	0.64
Pd <sub>3</sub> Fe	2.98	0.34	Ni <sub>3</sub> Fe <sup>c</sup>	2.91	0.60
Pd <sub>3</sub> Fe <sup>d</sup>	3.10	0.42	Ni <sub>3</sub> Fe <sup>c,d</sup>	2.97	0.62
PdFe	2.85	0.35	NiFe <sup>c</sup>	2.60	0.67
Pd <sub>3</sub> Co	1.97	0.48	Ni <sub>3</sub> Co	1.84	0.58
PdCo	1.97	0.35	NiCo	1.70	0.58

<sup>a</sup> Low and Collins (Ref. 14).

<sup>b</sup> Collins, Jones and Lowde (Ref. 13).

<sup>c</sup> Shull and Wilkinson (Ref. 12).

<sup>d</sup> Ordered alloy.

<sup>12</sup> C. G. Shull and M. K. Wilkinson, *Phys. Rev.* **97**, 304 (1955).

<sup>13</sup> M. F. Collins, R. V. Jones, and R. D. Lowde, *J. Phys. Soc. Japan* **17**, Suppl. B III, 19 (1962).

<sup>14</sup> G. E. Low and M. F. Collins, *J. Appl. Phys.* **34**, 1195 (1963).

is that the individual atomic moments remain nearly constant throughout. Thus, the Fe moment remains within 10% of  $2.8 \mu_B$  in both the Pd-Fe and Ni-Fe systems over a concentration range for which the average number of electrons per atom varies from 10–9. A similar property may be ascribed to the other atoms with characteristic moment values of  $1.8 \mu_B$  per Co,  $0.6 \mu_B$  per Ni and  $0.4 \mu_B$  per Pd. This atomic character of the moments in these face-centered cubic systems may well be explained by a partially localized-partially itinerant model. In this model the splitting of the  $d$  wave functions of  $t_{2g}$  and  $e_g$  symmetry is accomplished not by a true crystal field effect, but rather by the overlap properties in this crystal structure of the two types of wave functions. The strongly overlapping  $t_{2g}$  functions are assumed to form a conventional band, and the fractional moments are attributed to exchange splitting in that band. The  $e_g$  type functions do not

overlap appreciably in this crystal structure, and are assumed to remain localized. The electronic configurations  $e_g^2$ ,  $e_g^3$ , and  $e_g^4$  are then associated with integral moments of 2, 1, and 0  $\mu_B$  in Fe, Co, and Ni. These discrete moments associated with the  $e_g$  levels along with the partial moments from the  $t_{2g}$  band, which is similar for all of these atoms, are then responsible for the intrinsic atomic moments.

In the concentrated Pd-Fe and Pd-Co alloys the Pd moment remains nearly constant at  $0.4 \mu_B$  per atom, while in the dilute alloys this moment apparently assumes somewhat smaller values. It was mentioned in an earlier section that, in the dilute alloys, the Pd moment probably varies with distance from the Fe impurity atoms and that these apparent moments should be regarded as average values. Unfortunately, these data do not permit the evaluation of this Pd moment variation.

### Effect of Elevated Temperatures on Sputtering Yields\*

C. E. CARLSTON, G. D. MAGNUSON, A. COMEAUX, AND P. MAHADEVAN  
*Space Science Laboratory, General Dynamics/Convair, San Diego, California*  
 (Received 2 December 1964)

A study was made of the effect of elevated temperatures on the sputtering yields of polycrystalline and single-crystal metals. The temperature range extended from 350 to 1000°K. The yield determinations were made by standard weight-loss techniques. The bombarding ions were  $\text{Ar}^+$  with energies 2, 5, and 10 keV. The face-centered-cubic polycrystalline Cu and Al targets showed essentially no change in yield with temperature. This is to be contrasted with the polycrystalline body-centered-cubic targets Mo, W, and Ta which showed linear increases in yield of 26, 28, and 39%, respectively. A Mo(100) crystal face showed no change in yield over the temperature range, but a Mo(110) face showed a 12% increase in yield. On the other hand, a Cu(110) crystal showed no change in yield with temperature, while a Cu(111) face showed a decrease in yield of 24, 12, and 16% at 2, 5, and 10 keV, respectively.

#### INTRODUCTION

SOME measurements of sputtering yields have been made at elevated target temperatures. Almén and Bruce measured the sputtering yields of Ni, Pt, and Ag between 300 and 900°K when bombarded with 45-keV  $\text{Kr}^+$  ions.<sup>1</sup> They found that Ag had a constant sputtering yield  $S$  in atoms/ion, whereas Ni and Pt showed a monotonic decrease in  $S$  of about 30% over the temperature range of their experiments. Measurements<sup>2</sup> using 20-keV  $\text{Ar}^+$  ions bombarding polycrystalline Cu showed a slight increase of about 10% over the temperature range 300 to 600°K. Measurements<sup>3</sup> of

3-keV  $\text{N}_2^+$  ions bombarding polycrystalline Cu showed an approximate 15% decrease in sputtering yield over the temperature range 330 to 750°K. Wehner<sup>4</sup> has reported that the yields he has measured for polycrystalline materials bombarded by low-energy  $\text{Hg}^+$  ions change less than 15% over the temperature range 300 to 700°K.

At the other extreme of temperature there have recently been some measurements<sup>2</sup> made of Cu single crystals bombarded by 20-keV  $\text{Ar}^+$  and  $\text{Ne}^+$  ions at various temperatures between 30 and 320°K.

Various theoretical models have been proposed for the effect of temperature on the sputtering process. Two main lines of reasoning have been followed: annealing of the defects created by the bombardment, and disruption of focused collision sequences. Increased annealing of defects is expected as the target temperature is raised. This would tend to increase the sputtering

\* This research was supported in part by NASA, Lewis Research Center, Cleveland, Ohio.

<sup>1</sup> O. Almén and G. Bruce, *Nucl. Instr. Methods* **11**, 257 (1961).

<sup>2</sup> J. M. Fluitt, C. Snoek, and J. Kistemaker, *Physica* **30**, 144 (1964).

<sup>3</sup> T. W. Snouse and M. Bader, *Transactions of the Second International Vacuum Congress* (Pergamon Press, Inc., New York, 1962), Vol. 1, p. 271.

<sup>4</sup> G. K. Wehner, *Phys. Rev.* **108**, 35 (1957).